USC–SIPI REPORT #215

On Signal Sampling and Wavelet Coefficient Computation with Biorthogonal Wavelets

by

Xiang-Gen Xia, C.-C. Jay Kuo, and Zhen Zhang

September 1992

Signal and Image Processing Institute
UNIVERSITY OF SOUTHERN CALIFORNIA
Department of Electrical Engineering-Systems
3740 McClintock Avenue, Room 400
Los Angeles, CA 90089-2564 U.S.A.

Submitted to IEEE Transactions on Signal Processing.

On Signal Sampling and Wavelet Coefficient Computation with Biorthogonal Wavelets*

Xiang-Gen Xia† C.-C. Jay Kuo‡ Zhen Zhang†

September 4, 1992

Abstract

Several issues on signal sampling and wavelet coefficient computation for a continuous time signal with biorthogonal wavelet bases are studied in this research. Discrete wavelet transform (DWT) is often used to approximate wavelet series transform (WST) and continuous wavelet transform (CWT), since they can be computed numerically. We first estimate the approximation error of computed DWT coefficients by using the Mallat and Shensa algorithms, and show a procedure to design optimal FIR prefilters used in the Shensa algorithm to reduce the approximation error. Then, we examine a specific prefiltering process by which the computed DWT coefficients can be made exactly the same as the WST coefficients for signals belonging to the wavelet subspaces. A formula characterizing the aliasing error resulted from general signals with such a prefilter is also derived. Finally, numerical examples are presented to show the performance of the optimal FIR prefilters.

1 Introduction

Wavelet transforms have recently recognized as useful tools for various applications such as signal and image processing [1], [2], [3], [6], [8], [10], [11], [12], [16], [18], [23], [24], [27], [30], [32], [33], numerical analysis [4], [15], [17] and physics [22]. There are three types of wavelet transforms being discussed in the literature, namely, continuous wavelet transform (CWT) [12], wavelet series transform (WST) [9], [10], [13], [18], [19], [20], [21] and discrete wavelet transform (DWT) [25], [30]. These wavelet transforms based on biorthogonal wavelet bases

*This work was supported by the National Science Foundation Grant NCR-8905052 and a National Science Foundation Young Investigator Award.

†The authors are with Communication Science Institute, Department of Electrical Engineering-Systems, University of Southern California, Los Angeles, CA 90089-2565. E-mail: xianggen@irving.usc.edu and zzhang@solar.usc.edu

‡This author is with Signal and Image Processing Institute, Department of Electrical Engineering-Systems, University of Southern California, Los Angeles, CA 90089-2564. E-mail: cckuo@sipi.usc.edu

are briefly summarized below. For a more detailed discussion on definitions, properties and advantages of biorthogonal wavelets, we refer to [5], [7], [28] We will use the notation

$$f_{jk}(t) \triangleq 2^{j/2} f(2^j t - k), \quad j, k \in \mathbf{Z}, \qquad \text{and} \qquad f_{a,b}(t) = |a|^{-1/2} f(\frac{t-b}{a}), \quad a \neq 0, b \in \mathbf{R}.$$

Let $\psi(t)$ and $\tilde{\psi}(t)$ be, respectively, a real wavelet function and its dual such that $\{\psi_{jk}(t)\}_{j,k}$ and $\{\tilde{\psi}_{jk}(t)\}_{j,k}$ form a biorthogonal wavelet basis in $L^2(\mathbf{R})$. Then, for $f(t) \in L^2(\mathbf{R})$, its CWT with respect to the wavelet $\psi(t)$ is defined as

$$CWT\{f(t); a, b\} \triangleq \int_{-\infty}^{\infty} f(t)\psi_{a,b}(t)dt\,,$$

where a and b are called the scale and time parameters, respectively. The WST of $f(t)$ is obtained by sampling its CWT in the scale-time plane (a, b) with the so-called "dyadic" grid, i.e.

$$WST\{f(t); j, k\} = CWT\{f(t); a = 2^{-j}, b = k2^{-j}\}\,,\ j, k \in \mathbf{Z}\,.$$

Thus, the WST coefficients, also denoted by $b_{j,k}$, can be determined by

$$b_{j,k} \triangleq WST\{f(t); j, k\} = \int_{-\infty}^{\infty} f(t)\psi_{jk}(t)dt\,,\ j, k \in \mathbf{Z}\,. \tag{1.1}$$

Moreover, $f(t)$ can be reconstructed via

$$f(t) = \sum_j \sum_k b_{j,k}\tilde{\psi}_{jk}(t).$$

If the t as well as parameters (a, b) all take discrete values, which is recognized as a natural wavelet transform for the discrete-time signal $f(m\Delta t)$ with $m \in \mathbf{Z}$, the resulting transform is called the DWT of $f(t)$. It is clear that only the DWT coefficients can be computed numerically, and the CWT and WST coefficients have to be approximated by the DWT coefficients in practice.

Several numerical algorithms have been proposed to compute the DWT coefficients such as the Mallat algorithm [9], [18], [19], [20], [26], the "à trous" algorithm of Holschneider et al. [14], and the Shensa algorithm [23], [25] as a unified approach for the former two. The relationship of the Mallat and Shensa algorithms can be explained as follows. Let the sequence $x[n]$ be obtained by sampling a function $f(t) \in L^2(\mathbf{R})$, i.e. $x[n] = f(n\Delta t)$. Mallat [20] proposed an effective recursive algorithm to compute the DWT of $x[n]$ by implementing a recursion with cascaded quadrature mirror filter banks [29]. Shensa [23], [25] suggested to prefilter the sequence $x[n]$ by which the $x[n]$ is convolved with a sequence $q[n]$ to obtain

a new sequence $x'[n]$ and then the same recursion is applied to $x'[n]$. Thus, the Mallat algorithm can be viewed as a special case of the Shensa algorithm with $q[n]$ chosen to be the unit impulse sequence $\delta[n]$.

Efficient implementations and detailed computational complexity analysis for these algorithms were discussed by Rioul and Duhamel [23]. However, an important issue is the numerical accuracy of the computed DWT coefficients $b'_{j,k}$ with respect to the true WST coefficients $b_{j,k}$ as defined in (1.1). We [34], [35] have analyzed the error between $b_{j,k}$ and $b'_{j,k}$ for the case that the wavelet basis $\psi_{jk}(t)$ is orthonormal, i.e. $\psi_{jk}(t) = \tilde{\psi}_{jk}(t)$. In this research, the analysis is extended to the general biorthogonal case.

This paper is organized as follows. In Section 2, we review biorthogonal wavelet transforms and the Mallat and Shensa algorithms. An upper bound for the error between $b_{j,k}$ and the computed $b'_{j,k}$ by the Shensa algorithm is derived in Section 3 (see Proposition 3). Based on the error bound, we discuss the design of optimal prefilters for the Shensa algorithm in Section 4. Note that the computed DWT by the Shensa algorithm can also be interpreted as the exact WST of another continuous time signal $f'(t)$ obtained from $x[n]$ through a D/A converter $\chi(t)$. The optimal D/A converter is studied in the same section. Then, we show that there exists a class of signals whose computed DWT coefficients are exactly the same as the WST coefficients (see Propositions 5 and 6), and derive a bound for the aliasing error resulted from general signals not belonging to this class in Section 5 (see Propositions 8, 9 and 10). Numerical examples are given to demonstrate that the Shensa algorithm with optimal prefiltering is significantly better than the Mallat algorithm in Section 6.

2 Review of biorthogonal wavelets and discrete wavelet transform

2.1 Basic properties of biorthogonal wavelets

We review briefly basic properties of biorthogonal wavelets in this subsection. Most material covered can be found in the book by Chui [5]. Consider a real mother wavelet function $\psi(t)$, the associated scaling function $\phi(t)$, and their dual functions $\tilde{\psi}(t)$ and $\tilde{\phi}(t)$ such that $\{\psi_{jk}(t)\}_{j,k\in\mathbf{Z}}$ and $\{\tilde{\psi}_{jk}(t)\}_{j,k\in\mathbf{Z}}$ form a biorthogonal wavelet basis in $L^2(\mathbf{R})$. Let the Fourier transform of $f(t) \in L^2(\mathbf{R})$ be denoted by

$$\hat{f}(\omega) = \int_{-\infty}^{\infty} f(t)e^{-i\omega t}dt$$

and

$$H(\omega) = \sum_n h_n e^{-in\omega} \quad \text{and} \quad G(\omega) = \sum_n g_n e^{-in\omega}$$

be the associated filters of $\phi(t)$ and $\psi(t)$, respectively, such that they satisfy

$$\hat{\phi}(\omega) = H(\frac{\omega}{2})\hat{\phi}(\frac{\omega}{2}), \quad \text{and} \quad \hat{\psi}(\omega) = G(\frac{\omega}{2})\hat{\phi}(\frac{\omega}{2}).$$

Similarly, we associate the following dual filters

$$\tilde{H}(\omega) = \sum_n \tilde{h}_n e^{-in\omega} \quad \text{and} \quad \tilde{G}(\omega) = \sum_n \tilde{g}_n e^{-in\omega}$$

with the dual wavelet and scaling functions $\tilde{\psi}(t)$ and $\tilde{\phi}(t)$, respectively. One can derive the following well known properties for biorthogonal wavelets (see Chapter 5 in [5]):

$$\hat{\phi}(\omega) = \prod_{k=1}^{\infty} H(2^{-k}\omega), \quad \text{and} \quad \hat{\tilde{\phi}}(\omega) = \prod_{k=1}^{\infty} \tilde{H}(2^{-k}\omega), \tag{2.1}$$

$$\begin{cases} H(\omega)\overline{\tilde{H}(\omega)} + G(\omega)\overline{\tilde{G}(\omega)} = 1, \\ H(\omega)\overline{\tilde{H}(\omega+\pi)} + G(\omega)\overline{\tilde{G}(\omega+\pi)} = 0, \end{cases} \tag{2.2}$$

$$\sum_k \hat{\phi}(\omega + 2k\pi)\hat{\tilde{\phi}}(-\omega - 2k\pi) = 1, \tag{2.3}$$

and

$$\hat{\phi}(\omega) = \frac{\hat{\tilde{\phi}}(\omega)}{\sum_{k=-\infty} |\hat{\tilde{\phi}}(\omega + 2k\pi)|^2}. \tag{2.4}$$

Note that one possible solution for the second equation of the system (2.2) is

$$G(\omega) = e^{-i\omega}\overline{\tilde{H}(\omega+\pi)} \quad \text{and} \quad \tilde{G}(\omega) = e^{-i\omega}\overline{H(\omega+\pi)}, \tag{2.5}$$

which is often imposed to simplify the filter desgin procedure.

Let $(\tilde{V}_j)_{j\in\mathbf{Z}}$ denote the multiresolution wavelet subspaces in $L^2(\mathbf{R})$ corresponding to the dual scaling function $\tilde{\phi}(t)$, and $f_J(t)$ be the projection of $f \in L^2(\mathbf{R})$ in $\tilde{V}_J$ for an arbitrarily fixed integer J. In mathematical terms, we can write

$$f_J(t) = \sum_k c_{J,k}\tilde{\phi}_{Jk}(t) = \sum_{j<J}\sum_k b_{j,k}\tilde{\psi}_{jk}(t), \tag{2.6}$$

where

$$c_{J,k} = \int_{-\infty}^{\infty} f(t)\phi_{Jk}(t)dt, \tag{2.7}$$

and $b_{j,k}$ is defined in (1.1). The coefficients $b_{j,k}$ with $j < J$ can be obtained from $c_{J,k}$ via

$$c_{j-1,k} = \sqrt{2}\sum_n h_{n-2k}c_{j,n}, \tag{2.8}$$

and

$$b_{j-1,k} = \sqrt{2}\sum_n g_{n-2k}c_{j,n}. \tag{2.9}$$

for $j = J, J-1, \cdots, J_c+1$. Besides, one can reconstruct $c_{J,k}$ from $c_{J_c,k}$ and $b_{j,k}$, $J_c \le j \le J$, via

$$c_{j,n} = \sqrt{2}\left(\sum_k \tilde{h}_{n-2k}c_{j-1,k} + \sum_k \tilde{g}_{n-2k}b_{j-1,k}\right). \tag{2.10}$$

2.2 Mallat algorithm

We see from (2.8) and (2.9) that coefficients $b_{j,k}$ are related to $c_{J,k}$ through two filters H and G recursively. By examining the definition of $c_{J,k}$ in (2.7) and the lowpass property of the scaling function $\phi(t)$, one concludes that $c_{J,k}$ is close to $f(k/2^J)$ for sufficiently large J. Thus, it seems natural to replace $c_{J,k}$ with $f(k/2^J)$. To compute wavelet coefficients with the Mallat algorithm, we choose

$$c_{J,n}^{(M)} \triangleq x[n] = f(\frac{n}{2^J}).$$

and apply the recursion

$$c_{j-1,k}^{(M)} = \sqrt{2}\sum_n h_{n-2k}c_{j,n}^{(M)}, \tag{2.11}$$

$$b_{j-1,k}^{(M)} = \sqrt{2}\sum_n g_{n-2k}c_{j,n}^{(M)}, \tag{2.12}$$

for $j = J, J-1, \cdots, J_c+1$. The $b_{j,k}^{(M)}$ in (2.12) is called the wavelet coefficients obtained from the Mallat algorithm. The reconstruction formula (2.10) is also applicable for the reconstruction of $c_{J,k}^{(M)}$ from $c_{J_c,k}^{(M)}$ and $b_{j,k}^{(M)}$. The recursion in (2.11) and (2.12) stops at $j = J_c$ which corresponds to the coarsest resolution appropriate for a certain application. Without loss of generality, we let J_c approach to $-\infty$ so that the Mallat algorithm defines the discrete wavelet transform (DWT) for the sequence $x[n]$ [23], i.e.

$$DWT\{x[n]; j, k\} \equiv b_{j,k}^{(M)},\ j < J, k \in \mathbf{Z}.$$

The computed coefficients $b_{j,k}^{(M)}$ are in general not the same as the WST coefficients $b_{j,k}$ as given in (1.1). Their difference will be examined in Section 3 as a special case of the Shensa algorithm.

2.3 Shensa algorithm

To compute wavelet coefficients with the Shensa algorithm, we first perform a prefilering on the sampled signal $x[n] = f(n/2^J)$ to obtain a new sequence $x'[n]$, i.e.

$$x'[n] = \sum_m x[m]q[n-m], \tag{2.13}$$

and then apply the recursion (2.11) and (2.12) to $x'[n]$. The DWT coefficients of $x'[n]$, denoted by

$$DWT\{x'[n]; j, k\} \triangleq b_{j,k}^{(S)},\ j < J, k \in \mathbf{Z},$$

are called the wavelet coefficients obtained from the Shensa algorithm. Note that the computed wavelet coefficients $b_{j,k}^{(S)}$ are the WST coefficients of a certain continuous-time signal $f'(t)$. That is, we can write

$$2^{-J/2}x'[k] = \int_{-\infty}^{\infty} f'(t)\phi_{Jk}(t)dt, \tag{2.14}$$

so that

$$2^{-J/2}b_{j,k}^{(S)} = WST\{f'(t); j, k\}.$$

It has been shown in [23] that

$$f'(t) = \sum_n x[n]\chi(2^J t - n),$$

where $\chi(t)$ is a D/A converter (or interpolant) and related to the prefilter coefficients $q[n]$ via

$$q[n] = \int_{-\infty}^{\infty} \chi(t)\phi(t-n)dt\,. \tag{2.15}$$

It is clear that the only difference between the Mallat and Shensa algorithms is the prefiltering (2.13) adopted in the Shensa algorithm. Once initial sequences $x[n]$ and $x'[n]$ are given, the same recursion formulas (2.11) and (2.12) are applied for both algorithms. Thus, the Mallat algorithm can be viewed as a special case of the Shensa algorithm where $q[n]$ is the unit impulse sequence $\delta[n]$, and we will only examine the error between $b_{j,k}$ and $2^{-J/2}b_{j,k}^{(S)}$ for the Shensa algorithm in the following section.

3 Error estimation of computed wavelet coefficients

We see from the previous discussion that the difference between the WST coefficients $\{b_{j,k}\}$ and the DWT coefficients $\{2^{-J/2}b_{j,k}^{(S)}\}$ is resulted from the difference between the input

sequences $c_{J,k}$ in (2.7) and $2^{-J/2}x'[k]$. This can be written as

$$e_{j,k} \triangleq b_{j,k} - 2^{-J/2}b_{j,k}^{(S)} = DWT\{c_{J,n} - 2^{-J/2}x'[n]; j, k\}. \tag{3.1}$$

An estimate of the difference between $\{c_{J,k}\}_{k\in\mathbf{Z}}$ and $\{2^{-J/2}x'[k]\}_{k\in\mathbf{Z}}$ is given below.

Proposition 1 *For $k \in \mathbf{Z}$,*

$$c_{J,k} - 2^{-J/2}x'[k] = \frac{2^{J/2}}{2\pi}\int_{-\infty}^{\infty} \hat{f}(-2^J\omega)(\hat{\phi}(\omega) - Q(\omega))e^{-ik\omega}d\omega\,. \tag{3.2}$$

where

$$Q(\omega) = \sum_n q[n]e^{in\omega}$$

Proof: See Appendix A.1. □

In particular, if $f(t)$ is $2^J\pi$ band-limited, i.e., $\hat{f}(\omega) = 0$ for $|\omega| > 2^J\pi$, we have the following corollary.

Corollary 1 *If $f(t)$ is $2^J\pi$ band-limited,*

$$\sum_k |c_{J,k} - 2^{-J/2}x'[k]|^2 = \frac{2^{J-1}}{\pi}\int_{-\pi}^{\pi} |\hat{f}(-2^J\omega)|^2|Q(\omega) - \hat{\phi}(\omega)|^2 d\omega. \tag{3.3}$$

Proof: When $f(t)$ is $2^J\pi$ band-limited, (3.2) becomes

$$c_{J,k} - 2^{-J/2}x'[k] = \frac{2^{J/2}}{2\pi}\int_{-\pi}^{\pi} \hat{f}(-2^J\omega)(\hat{\phi}(\omega) - Q(\omega))e^{-ik\omega}d\omega\,,$$

for all $k \in \mathbf{Z}$. Then, by using the Parseval equality, (3.3) is proved. □

Equation (3.3) gives a precise formula for the error between $c_{J,k}$ and $2^{-J/2}x'[k]$ in terms of the prefilter characteristic $Q(\omega)$, which therefore plays a key role in reducing the error $e_{j,k}$. By using (3.3) and (2.15), one can also formulate the error in terms of the D/A converter $\chi(t)$ as follows.

Corollary 2 *If $f(t)$ is $2^J\pi$ band-limited,*

$$\sum_k |c_{J,k} - 2^{-J/2}x'[k]|^2 = \frac{2^{J-1}}{\pi}\int_{-\pi}^{\pi} |\hat{f}(-2^J\omega)|^2|A(\omega) - \hat{\phi}(\omega)|^2 d\omega\,, \tag{3.4}$$

where

$$A(\omega) \triangleq \sum_m \hat{\phi}(\omega + 2m\pi)\hat{\chi}(-\omega - 2m\pi). \tag{3.5}$$

A direct consequence of Corollary 2 is that if the D/A converter $\chi(t)$ is chosen to be the sinc function, $c_{J,k}$ is exactly the same as $2^{-J/2}x'[k]$ for all k so that $b_{j,k} = 2^{-J/2}b_{j,k}^{(S)}$ for $j < J, k \in \mathbf{Z}$. However, for $\chi(t)$ to be the sinc function, the corresponding prefilter sequence $q[n]$ as given in (2.15) has an infinite duration.

Based on the error estimate in terms of a filter characteristic $Q(\omega)$ as given in Proposition 1, we are ready to estimate the error $e_{j,k}$ between $b_{j,k}$ and $2^{-J/2}b_{j,k}^{(S)}$. The key is the analysis of the recursive procedures as given by (2.11) and (2.12). Let $s[n]$ be an arbitrary discrete sequence used as the input to the filters $H(\omega)$ and $G(\omega)$ so that it is decomposed into an approximation sequence $a[n]$ and a detail sequence $d[n]$:

$$a[k] = \sqrt{2}\sum_n h_{n-2k}s[n], \tag{3.6}$$

and

$$d[k] = \sqrt{2}\sum_n g_{n-2k}s[n]. \tag{3.7}$$

We have the following proposition.

Proposition 2

$$\sum_n |a[n]|^2 + \sum_n |d[n]|^2 \le C_{\max}\sum_n |s(n)|^2,$$

where

$$C_{\max} = \max_{\omega\in[-\pi,\pi]}\left(|H(\omega)|^2 + |G(\omega)|^2\right) + \max_{\omega\in[-\pi/2,\pi/2]}\left|\mathrm{Re}(\overline{H(\omega)}H(\omega+\pi) + \overline{G(\omega)}G(\omega+\pi))\right|. \tag{3.8}$$

In particular, if

$$\begin{cases} |H(\omega)|^2 + |G(\omega)|^2 &= 1, \\ \mathrm{Re}(\overline{H(\frac{\omega}{2})}H(\frac{\omega}{2}+\pi) + \overline{G(\frac{\omega}{2})}G(\frac{\omega}{2}+\pi)) &= 0, \end{cases} \quad \forall\omega\in[-\pi,\pi], \tag{3.9}$$

then

$$\sum_n |a[n]|^2 + \sum_n |d[n]|^2 = \sum_n |s[n]|^2. \tag{3.10}$$

Thus, the decomposition (3.6)-(3.7) preserves energy.

Proof: See Appendix A.2. □

For othorgonal wavelets, since $H(\omega) = \tilde{H}(\omega)$ and $G(\omega) = \tilde{G}(\omega)$, (3.9) holds as a direct consequence of (2.2). However, the identity (3.9) in general fails for biorthogonal wavelets so that the decomposition process does not preserve the energy and it is difficult to derive a precise error formula for the norm of $e_{j,k}$ as done in [35]. We will instead derive an upper bound for the error estimate.

Proposition 3 *If $f(t)$ is $2^J\pi$ band-limited, then*

$$\sum_k |c_{J-1,k} - 2^{-J/2}c_{J-1,k}^{(S)}|^2 + \sum_k |e_{J-1,k}|^2 \le C_{\max}\frac{2^{J-1}}{\pi}\int_{-\pi}^{\pi} |\hat{f}(-2^J\omega)|^2|Q(\omega) - \hat{\phi}(\omega)|^2 d\omega\,, \tag{3.11}$$

and

$$\sum_k |e_{j-1,k}|^2 \le C_{\max}\sum_k |c_{j,k} - 2^{-J/2}c_{j,k}^{(S)}|^2, \quad \text{for} \quad j \le J-1, \tag{3.12}$$

where $e_{j,k}$ is defined in (3.1) and $C_{\max}$ is given in (3.8). Furthermore, if (3.9) is true, then

$$\sum_{j<J}\sum_k |b_{j,k} - 2^{-J/2}b_{j,k}^{(S)}|^2 = \frac{2^{J-1}}{\pi}\int_{-\pi}^{\pi} |\hat{f}(-2^J\omega)|^2|Q(\omega) - \hat{\phi}(\omega)|^2 d\omega. \tag{3.13}$$

Proof: This proposition can be derived directly from

$$\begin{aligned} c_{j-1,k} - 2^{-J/2}c_{j-1,k}^{(S)} &= \sqrt{2}\textstyle\sum_n h_{n-2k}(c_{j,n} - 2^{-J/2}c_{j,n}^{(S)}), \\ e_{j-1,k} &= \sqrt{2}\textstyle\sum_n g_{n-2k}(c_{j,n} - 2^{-J/2}c_{j,n}^{(S)}), \end{aligned} \tag{3.14}$$

(3.4) and Proposition 2. □

By recursively applying the error bound (3.12) to (3.14), we obtain another error bound for computed wavelet coefficients with respect to a $2^J\pi$ band-limited signal $f(t)$ and $j < J$, i.e.

$$e_j \triangleq \sum_k |b_{j,k} - 2^{-J/2}b_{j,k}^{(S)}|^2 \le C_{\max}^{J-j}\frac{2^{J-1}}{\pi}\int_{-\pi}^{\pi} |\hat{f}(-2^J\omega)|^2|Q(\omega) - \hat{\phi}(\omega)|^2 d\omega. \tag{3.15}$$

By examining (3.13) and (3.15), we may conclude that for a signal with energy concentrated in frequency band $[-2^J\pi, 2^J\pi]$, the integral term

$$C_{f,\phi}(Q) = \int_{-\pi}^{\pi} |\hat{f}(-2^J\omega)|^2|Q(\omega) - \hat{\phi}(\omega)|^2 d\omega \tag{3.16}$$

is the dominant term of the error. Thus, it is natural to minimize $C_{f,\phi}(Q)$ for the design of prefilter $Q(\omega)$ to reduce the error $e_{j,k}$.

4 Optimal FIR prefilter design for Shensa algorithm

4.1 Determination of optimal FIR prefilter

In this section, we consider the determination of the optimal filter $q_o[n]$ (or $Q_o(\omega)$) which has a finite length and minimizes the cost function $C_{f,\phi}(Q)$ as given in (3.16). To do so, let

us expand $C_{f,\phi}(Q)$ as a function of $q[n]$ as follows.

$$\begin{aligned} C_{f,\phi}(Q) &= \int_{-\pi}^{\pi} |\hat{f}(-2^J\omega)|^2 |\sum_n q[n]e^{in\omega} - \hat{\phi}(\omega)|^2 d\omega \\ &= A\sum_n q^2[n] - \sum_{n<m} B_{nm}q[n]q[m] + \sum_n C_n q[n] + D\,, \end{aligned}$$

where

$$A = \int_{-\pi}^{\pi} |\hat{f}(-2^J\omega)|^2 d\omega, \tag{4.1}$$

$$B_{nm} = 2\int_{-\pi}^{\pi} |\hat{f}(-2^J\omega)|^2 \cos((n-m)\omega) d\omega, \text{ for } n \neq m, \tag{4.2}$$

$$C_n = \int_{-\pi}^{\pi} |\hat{f}(-2^J\omega)|^2 \mathrm{Re}(\hat{\phi}(\omega)e^{-in\omega}) d\omega, \tag{4.3}$$

and

$$D = \int_{-\pi}^{\pi} |\hat{f}(-2^J\omega)|^2 |\hat{\phi}(\omega)|^2 d\omega. \tag{4.4}$$

The solution of the above problem can be solved from the following equations:

$$\frac{\partial C_{f,\phi}(Q)}{\partial q[n]} = 0, \text{ for } n \in \mathbf{Z}. \tag{4.5}$$

Let the prefilter be an FIR filter of length N with filter coefficients $q[n] = 0$ for $n < N_1$ and $n \geq N_2$ and $N_2 - N_1 = N > 0$. Then, with (4.5), one can show that the optimal $q_o[n]$, $N_1 \leq n \leq N_2 - 1$, can be solved from the following linear equations:

$$\mathbf{T_1 q_o} = \mathbf{C_1}, \tag{4.6}$$

where $\mathbf{T_1} = (t_{nm})_{N_1 \leq n,m < N_2}$ with

$$t_{nm} = \begin{cases} 2A, & n = m, \\ -B_{nm}, & n \neq m, \end{cases}$$

$$\mathbf{C_1} = (-C_{N_1}, -C_{N_1+1}, \cdots, -C_{N_2-2}, -C_{N_2-1})^t,$$

$$\mathbf{q_o} = (q_o[N_1], q_o[N_1+1], \cdots, q_o[N_2-2], q_o[N_2-1])^t,$$

and A, B_{nm} and C_n are defined by (4.1), (4.2) and (4.3), respectively.

For some applications, it may be preferable that the prefilter does not depend on a signal while some partial knowledge of signals is available, say, the rough shape of signal spectra. To compute the WST coefficients for this class of signals, we may adopt a procedure using a nonnegative weighting function $F(\omega)$ to replace the term $|\hat{f}(-2^J\omega)|^2$ in (3.16). For example, consider

$$F(\omega) = e^{-a\omega^2}\,, a \geq 0. \tag{4.7}$$

where the parameter a can be adjusted according to different applications. If the input signal is known in advance, it is natural that the error $b_{j,k}^{(S)}$ resulted from the signal-independent optimal prefilter is larger than that resulted from a signal-dependent optimal prefilter. Their performance comparison will be given in Section 5.

4.2 Determination of the optimal D/A converter

In Section 4.1, we discussed the optimal prefilter $q_o[n]$ with a fixed length N minimizing the cost function $C_{f,\phi}(Q)$. In this section, we will examine the optimal D/A converter $\chi_o(t)$ associated with the optimal prefilter. Recall (2.15) for the relation between $\chi(t)$ and $q[n]$. Now, we define

$$q(s) = \int_{-\infty}^{\infty} \chi(t)\phi(t-s)dt, \ s \in \mathbf{R}$$

so that $q[n] = q(n)$ for all $n \in \mathbf{Z}$. In other words, $q(s)$ is a continuous-time signal which interpolates $q[n]$ at interger points. Let $\hat{q}(\omega)$ be the Fourier transform of $q(s)$. Then, we have

$$\hat{q}(\omega) = \hat{\chi}(\omega)\hat{\phi}(-\omega), \ \omega \in \mathbf{R}. \tag{4.8}$$

Thus, given $q(s)$, $\hat{\chi}(\omega)$ can be solved if $\hat{\phi}(-\omega) \neq 0$.

In the following, we assume that the scaling function satisfies

$$\hat{\phi}(\omega) \neq 0, \ \text{for } |\omega| < \pi, \tag{4.9}$$

which is equivalent to

$$H(\omega) \neq 0, \ \text{for } |\omega| < \pi/2$$

due to (2.1). The scaling functions of most common wavelets satisfy (4.9). One possible choice of $q(s)$ is

$$q(s) = \sum_n q[n] \frac{\sin \pi(s-n)}{\pi(s-n)}. \tag{4.10}$$

Since there is only a finite number of nonzero coefficients in $q[n]$, $q(s)$ in (4.10) is a π band-limited signal so that (4.8) holds for $\omega \in [-\pi, \pi]$. This implies that, with respect to the optimal $q_o[n]$, an optimal D/A converter $\chi_o(t)$ can be obtained from its Fourier transform

$$\hat{\chi}_o(\omega) = \frac{Q_o(-\omega)}{\hat{\phi}(-\omega)} \chi_{[-\pi,\pi]}(\omega), \tag{4.11}$$

where $\chi_{[a,b]}(\omega)$ denotes the indicator function which is equal to 1 when $\omega \in [a,b]$ and 0 otherwise and $Q_o(-\omega) = \sum_n q_o[n]e^{-in\omega}$. Thus, we prove the following proposition.

Proposition 4 *For the optimal prefilter $q_o[n]$ in (4.6), the $\chi_o(t)$ satisfying (4.11) is a corresponding D/A converter in (2.15) for the Shensa algorithm.*

It is worthwhile to comment that the $\chi_o(t)$ satisfying (4.11) is however not the unique solution to (2.15) for a given $q_o[n]$.

5 Sampling and aliasing error estimation

5.1 A sufficient condition for error-free WST coefficient computation

We showed in Section 3 that the WST coefficients of a $2^J\pi$ band-limited signal can be exactly computed by using the Shensa algorithm with the interpolant $\chi(t)$ being the sinc function. In this subsection, we present another class of signals whose WST coefficients can be exactly obtained from the DWT of their samples. In the following, we assume that the dual function $\tilde{\phi}(t)$ is real and continuous and satisfies

a). $\tilde{\phi}(t) = O(|t|^{-1-\epsilon})$ as $t \to \pm\infty$, $t \in \mathbf{R}$,

b). $\tilde{\Phi}(\omega) = \sum_n \hat{\tilde{\phi}}(\omega + 2k\pi) \neq 0, \omega \in \mathbf{R}$.

Let $\{\tilde{V}_j\}_{j\in\mathbf{Z}}$ be the multiresolution analysis of $L^2(\mathbf{R})$ corresponding to $\tilde{\phi}(t)$, i.e., for each $j \in \mathbf{Z}$,

$$\tilde{V}_j = \text{closure}\{\text{linear span}\{\tilde{\phi}_{jk}(t) : k \in \mathbf{Z}\}\}\,.$$

Then, the Walter sampling theorem [31] for orthogonal wavelet subspaces can be easily extended to biorthogonal wavelet subspaces. The generalized sampling theorem is stated as follows.

Proposition 5 *Let the dual function $\tilde{\phi}(t)$ be real and continuous, and satisfy the above conditions (a) and (b). Besides, the interpolant $\chi(t)$ has the Fourier transform*

$$\hat{\chi}(\omega) = \frac{\hat{\tilde{\phi}}(\omega)}{\tilde{\Phi}(\omega)}\,, \tag{5.1}$$

and $\sum_n |f(n/2^J)|^2 < \infty$ for some integer J. Then, $f(t) \in \tilde{V}_J$ if and only if

$$f(t) = \sum_n f(\frac{n}{2^J})\chi(2^J t - n)\,. \tag{5.2}$$

For the rest of this section, we assume the interpolant $\chi(t)$ of the form (5.1). Based on Proposition 5, we have a straightforward corollary.

Corollary 3 *If $f(t) \in \tilde{V}_J$ for some integer $J > 0$, then the WST coefficients of $f(t)$ can be exactly computed from the Shensa algorithm with the scaling function $\phi(t)$, that is,*

$$WST\{f(t); j, k\} = 2^{-J/2} DWT\{x'[n]; j, k\}\,,\ j < J, k \in \mathbf{Z}\,.$$

Since $\tilde{V}_J$ approaches $L^2(\mathbf{R})$ as J goes to infinity, $\tilde{V}_J$ provides a suitable model to approximate $L^2(\mathbf{R})$ for large J. However, it is in general difficult to verify the condition $f(t) \in \tilde{V}_J$ for a given finite J so that Proposition 5 has its limitation in practice. We now present a condition which is more general and easier to verify.

Proposition 6 *If the interpolant $\chi(t)$ satisfies (5.1), then the following two statements are equivalent:*
(i) $f(t) \in L^2(\mathbf{R})$ satisfies the condition

$$\int_{-\infty}^{\infty} \hat{f}(-2^J\omega)(\hat{\phi}(\omega) - \frac{1}{\bar{\Phi}(-\omega)})e^{-ik\omega}d\omega = 0\,,\ \forall\, k \in \mathbf{Z}\,. \tag{5.3}$$

(ii) The WST coefficients of $f(t)$ can be exactly computed from the Shensa algorithm with the scaling function $\phi(t)$, i.e., $b_{j,k} = 2^{-J/2} b_{j,k}^{(S)}$, $j < J, k \in \mathbf{Z}$.

Proof: See Appendix A.3. □

The following proposition tells us that condition (5.3) in Proposition 6 is more general than that given in Proposition 5.

Proposition 7 *If $f(t) \in \tilde{V}_J$, then $f(t)$ satisfies (5.3). But, the converse is not true in general.*

Proof: See Appendix A.4. □

5.2 Aliasing error estimation

For a general signal $f(t)$ not necessarily satisfying (5.3), $b_{j,k}$ may be not equal to $2^{-J/2} b_{j,k}^{(S)}$ even if $\chi(t)$ is of the form (5.1). It is because that the aliasing error $f(t) - f'(t)$ may occur where

$$f'(t) = \sum_k f(\frac{k}{2^J})\chi(2^J t - k).$$

In the following, we always assume that $\sum_k |f(k/2^J)|^2 < \infty$ to guarantee $f'(t) \in L^2(\mathbf{R})$. The objective of this subsection is to estimate $\|f - f'\|$. To do so, we first need a result proved in [36]. Let $U_J(\epsilon)$ be the signal set

$$U_J(\epsilon) \triangleq \left\{ f(t) \in L^2(\mathbf{R}) : \int_{\mathbf{R}-[-2^J\pi, 2^J\pi]} |\hat{f}(\omega)|^2 d\omega \le \epsilon^2 \right\}. \tag{5.4}$$

Then, we have the following property.

Proposition 8 *If $f(t) \in U_J(\epsilon)$ for some $\epsilon \geq 0$, then*

$$B_1(f,\phi,\tilde{\phi}) - (1+C)\frac{1}{\sqrt{2\pi}}\epsilon \leq \|f - f_J\| \leq B_1(f,\phi,\tilde{\phi}) + (1+C)\frac{1}{\sqrt{2\pi}}\epsilon,$$

where

$$B_1(f,\phi,\tilde{\phi}) = \sqrt{\frac{2^{J-1}}{\pi}}\left(\int_{-\pi}^{\pi} |\hat{f}(-2^J\pi)|^2(1 - |\hat{\phi}(\omega)\hat{\tilde{\phi}}(\omega)|)d\omega\right)^{1/2}, \tag{5.5}$$

$$\begin{aligned} C &= \left[\max_{\omega\in[-\pi,\pi]} \sum_k |\hat{\phi}(\omega+2k\pi)|^2 \max_{\omega\in[-\pi,\pi]} \sum_k |\hat{\tilde{\phi}}(\omega+2k\pi)|^2\right]^{1/2} \\ &= \left[\max_{\omega\in[-\pi,\pi]} \frac{\hat{\phi}(\omega)}{\hat{\tilde{\phi}}(\omega)} \max_{\omega\in[-\pi,\pi]} \frac{\hat{\tilde{\phi}}(\omega)}{\hat{\phi}(\omega)}\right]^{1/2}, \end{aligned} \tag{5.6}$$

and $f_J(t)$ is the projection in (2.6) of $f(t)$ in $\tilde{V}_J$.

Proof: See the proof of Theorem 1 in [36]. □

Since $\{\chi(2^Jt - n)\}_n$ is a basis of $\tilde{V}_J$ (see Walter [31]), we know that $f'(t) \in \tilde{V}_J$. We decompose the error $\|f - f'\|$ into two parts: the high resolution error $\|f - f_J\|$ and the low resolution error $\|f_J - f'\|$. If the wavelet basis is orthonormal,

$$\|f - f'\|^2 = \|f - f_J\|^2 + \|f_J - f'\|^2.$$

We now state an upper bound result for the error estimate.

Proposition 9 *If $f(t) \in U_J(\epsilon)$ for some $\epsilon \geq 0$, then*

$$\|f - f'\| \leq B_1(f,\phi,\tilde{\phi}) + C_1B_2(f,\phi,\tilde{\phi}) + (1+C)\frac{1}{\sqrt{2\pi}}\epsilon, \tag{5.7}$$

where $B_1(f,\phi,\tilde{\phi})$ is defined by (5.5),

$$B_2(f,\phi,\tilde{\phi}) = \sqrt{\frac{2^{J-1}}{\pi}}\left[\sum_k \left|\int_{-\infty}^{\infty} \hat{f}(-2^J\omega)\left(\hat{\phi}(\omega) - \frac{1}{\hat{\tilde{\Phi}}(-\omega)}\right)e^{-ik\omega}d\omega\right|^2\right]^{1/2}, \tag{5.8}$$

$$C_1 = \left(\max_{\omega\in[-\pi,\pi]} \sum_k |\hat{\tilde{\phi}}(\omega+2k\pi)|^2\right)^{1/2} = \left(\max_{\omega\in[-\pi,\pi]} \frac{\hat{\tilde{\phi}}(\omega)}{\hat{\phi}(\omega)}\right)^{1/2}, \tag{5.9}$$

and C is the constant in (5.6).

Proof: See Appendix A.5. □

When $f(t)$ is $2^J\pi$ band-limited, we know from (5.4) that $\epsilon = 0$ so that the above proposition can be simplified.

Corollary 4 *If $f(t)$ is $2^J\pi$ band-limited so that $f(t) \in U_J(\epsilon)$ with $\epsilon = 0$, then*

$$\|f - f'\| \leq B_1(f, \phi, \tilde{\phi}) + C_1 B_3(f, \phi, \tilde{\phi}), \tag{5.10}$$

where $B_1(f, \phi, \tilde{\phi})$ is defined by (5.5),

$$B_3(f, \phi, \tilde{\phi}) = \sqrt{\frac{2^{J-1}}{\pi}} \left[\frac{1}{2\pi} \int_{-\pi}^{\pi} |\hat{f}(-2^J\omega)|^2 \left| \hat{\phi}(\omega) - \frac{1}{\bar{\tilde{\Phi}}(-\omega)} \right|^2 d\omega \right]^{1/2},$$

and C_1 is the constant in (5.9). Moreover, if the wavelet basis is orthonormal, then $C_1 = 1$ and

$$\|f - f'\|^2 = (B_1(f, \phi, \tilde{\phi}))^2 + (B_3(f, \phi, \tilde{\phi}))^2.$$

Note that the upper bound in (5.7) involves two functions $B_1(f, \phi, \tilde{\phi})$ and $B_2(f, \phi, \tilde{\phi})$. For biorthogonal wavelet basis, it is possible to derive another upper bound for the estimate of $\|f - f'\|$ involving $B_1(f, \phi, \tilde{\phi})$ only as stated below.

Proposition 10 *If $f(t) \in U_J(\epsilon)$ for some $\epsilon \geq 0$, then*

$$\|f - f'\| \leq (1 + C_2) B_1(f, \phi, \tilde{\phi}) + (1 + C_2)(1 + C) \frac{1}{\sqrt{2\pi}} \epsilon, \tag{5.11}$$

where $B_1(f, \phi, \tilde{\phi})$ is given by (5.5),

$$C_2 = \max_{\omega \in [-\pi, \pi]} \frac{(\sum_k |\hat{\tilde{\phi}}(\omega + 2k\pi)|^2)^{1/2}}{|\bar{\tilde{\Phi}}(\omega)|} = \max_{\omega \in [-\pi, \pi]} \left(\frac{\hat{\tilde{\phi}}(\omega)}{\hat{\phi}(\omega)} \right)^{1/2} \frac{1}{|\bar{\tilde{\Phi}}(\omega)|}. \tag{5.12}$$

and C is the constant in (5.6).

Proof: See Appendix A.6. □

Besides, an immediate consequence of Proposition 10 applied to $2^J\pi$ band-limited signals can be stated as follows.

Corollary 5 *If $f(t)$ is $2^J\pi$ band-limited, then*

$$\|f - f'\| \leq (1 + C_2) B_1(f, \phi, \tilde{\phi}). \tag{5.13}$$

Finally, since

$$\begin{aligned}\sum_{j<J}\sum_{k}|b_{j,k}-2^{-J/2}b_{j,k}^{(S)}|^2 &= \sum_{j<J}\sum_{k}|b_{j,k}-WST\{f'(t);j,k\}|^2\\ &= \sum_{j<J}\sum_{k}\left|\int_{-\infty}^{\infty}f(t)\psi_{j,k}(t)dt-\int f'(t)\psi_{j,k}(t)dt\right|^2\\ &\leq D\|f-f'\|^2,\end{aligned}$$

where D is a positive constant only depending on the basis, all estimates derived for $\|f-f'\|$ such as (5.7), (5.10), (5.11) and (5.13) can in fact be used as a bound for $|b_{j,k}-2^{-J/2}b_{j,k}^{(S)}|$.

6 Numerical Examples

Numerical examples are given below to show the performance of the optimal prefilters designed in Section 4 for biorthogonal wavelets. Similar study has been performed for the orthogonal case in [34]. The biorthogonal wavelet basis adopted here is given in [7]. The filters are

$$H(\omega)=\left(\frac{1+e^{-i\omega}}{2}\right)^2, \quad \text{and} \quad \tilde{H}(\omega)=\left(\frac{1+e^{i\omega}}{2}\right)^2 e^{-2i\omega}(1+2\sin^2(\frac{\omega}{2})),$$

and filters $G(\omega)$ and $\tilde{G}(\omega)$ are determined according to (2.5). The graphs of $|H(\omega)|^2+|G(\omega)|^2$ and $\mathrm{Re}\left((\overline{H(\omega)}H(\omega+\pi)+\overline{G(\omega)}G(\omega+\pi)\right)$ are plotted in Figure 1. We see from the figure that the constant $C_{\max}$ in Proposition 3 is $1.5+0.75=2.25$ so that the discrete wavelet transform does not preserve the energy of input discrete time signals. The test function considered is

$$f(t)=\frac{\sin(2^6\pi t)}{\pi t},$$

which is $2^J\pi$ band-limited with $J=6$. We focus on noncausal filters $q(-N_1), q(-N_1+1),...,q(N_1-1),q(N_1)$ of length $N=2N_1+1$, and both signal dependent and signal independent optimal prefilters are designed. For the signal independent case, we choose the weighting function

$$F(\omega)=e^{-a\omega^2}, \quad a=0.01.$$

Tables 1 and 2 show the filter coefficients for N_1 ranging from 0 to 5.

The errors e_j, $j=5,4,3$, between the true WST coefficients and the computed ones are defined as

$$e_5 = \sum_{k=-120}^{120}|b_{5,k}-\frac{1}{8}b_{5,k}^{(S)}|^2,$$

length N_1	$q_o[n], -N_1 \leq n \leq N_1$					
0	1.0000					
1	0.6766	0.4347	-0.0976			
2	-0.0783	0.6766	0.4347	-0.0976	0.0573	
3	0.0518	-0.0783	0.6766	0.4347	-0.0976	0.0573
	-0.0405					
4	-0.0379	0.0518	-0.0783	0.6766	0.4347	-0.0976
	0.0573	-0.0405	0.0314			
5	0.0298	-0.0379	0.0518	-0.0783	0.6766	0.4347
	-0.0976	0.0573	-0.0405	0.0314	-0.0256	

Table 1: Signal dependent optimal prefilters for the test function $f(t)$

length N_1	$q_o[n], -N_1 \leq n \leq N_1$					
0	1.0000					
1	0.6749	4349	-0.0965			
2	-0.0770	0.6763	0.4348	-0.0974	0.0563	
3	0.0508	-0.0780	0.6765	0.4347	-0.0976	0.0571
	-0.0397					
4	-0.0371	0.0516	-0.0782	0.6766	0.4347	-0.0976
	0.0572	-0.0403	0.0307			
5	0.0291	-0.0377	0.0517	-0.0782	0.6766	0.4347
	-0.0976	0.0572	-0.0404	0.0312	-0.0250	

Table 2: Signal independent optimal prefilters with weighting function for $a = 0.01$

$$e_4 = \sum_{k=-60}^{60} |b_{4,k} - \frac{1}{8} b_{4,k}^{(S)}|^2,$$

$$e_3 = \sum_{k=-30}^{30} |b_{3,k} - \frac{1}{8} b_{3,k}^{(S)}|^2.$$

and plotted in Figure 2. Recall that the Shensa algorithm with the prefilter of length 1 is in fact the Mallat algorithm. Thus, we see a clear advantage of the Shensa algorithm with optimal prefilters of even very short length. There is no substantial difference for signal dependent and signal independent cases if an appropriate parameter a of the weighting function in (4.7) is used for this particular test problem. In Figure 3, we show the corresponding optimal D/A converter $\chi_o(t)$ with respect to $Q_o(\omega)$ in Tables 1 and 2 with lengthes 3 and 5.

7 Concluding remarks

In this paper, we studied the error estimate between the true WST coefficients and the computed ones from samples of a continuous time signal by using the Shensa algorithm with biorthogonal wavelet bases. We discussed the design of optimal prefilters used in the Shensa algorithm, and showed that they provide significant improvement on the accuracy of computed wavelet coefficients over the Mallat algorithm. A related issue with prefiltering is the interpolation of samples of a continuous time signal. The accuracy of the interpolated signal via sampled points plays a key role for the error estimate of computed WST coefficients. Optimal interpolants corresponding to optimal prefilters were also discussed. Finally, we considered the generalization of the Walter sampling theorem for signals in biorthogonal wavelet subspaces, and examined several error bounds for the aliasing error if signals to be sampled are not necessarily in wavelet subspaces.

Appendices

A.1 Proof of Proposition 1:

Since

$$\begin{aligned} 2^{-J/2}x'[k] &= 2^{-J/2}\sum_m x[m]q[k-m] \\ &= 2^{-J/2}\sum_m \frac{1}{2\pi}\int_{-\infty}^{\infty}\hat{f}(\omega)e^{i\omega m/2^J}d\omega q[k-m] \\ &= \frac{2^{J/2}}{2\pi}\int_{-\infty}^{\infty}\hat{f}(2^J\omega)\sum_m e^{i\omega m}d\omega q[k-m] \\ &= \frac{2^{J/2}}{2\pi}\int_{-\infty}^{\infty}\hat{f}(2^J\omega)\sum_m e^{i\omega(m-k)}q[k-m]e^{i\omega k}d\omega \\ &= \frac{2^{J/2}}{2\pi}\int_{-\infty}^{\infty}\hat{f}(-2^J\omega)Q(\omega)e^{-i\omega k}d\omega\,, \end{aligned}$$

and

$$\begin{aligned} c_{J,k} &= 2^{J/2}\int_{-\infty}^{\infty}f(t)\phi(2^Jt-k)dt \\ &= 2^{J/2}\int_{-\infty}^{\infty}f(t)\frac{1}{2\pi}\int_{-\infty}^{\infty}\hat{\phi}(\omega)e^{i\omega(2^Jt-k)}d\omega dt \\ &= \frac{2^{J/2}}{2\pi}\int_{-\infty}^{\infty}(\int_{-\infty}^{\infty}f(t)e^{i\omega 2^Jt}dt)\hat{\phi}(\omega)e^{-i\omega k}d\omega \\ &= \frac{2^{J/2}}{2\pi}\int_{-\infty}^{\infty}\hat{f}(-2^J\omega)\hat{\phi}(\omega)e^{-i\omega k}d\omega\,. \end{aligned}$$

Thus, (3.2) is proved. □

A.2 Proof of Proposition 2:

Let $S(\omega)=\sum_n s[n]e^{-in\omega}$. Take Fourier transforms of (3.6) and (3.7),

$$A(2\omega)=\frac{1}{\sqrt{2}}\left[\overline{H(\omega)}S(\omega)+\overline{H(\omega+\pi)}S(\omega+\pi)\right],$$

and

$$D(2\omega)=\frac{1}{\sqrt{2}}\left[\overline{G(\omega)}S(\omega)+\overline{G(\omega+\pi)}S(\omega+\pi)\right].$$

Therefore,

$$\sum_n |a[n]|^2+\sum_n |d[n]|^2$$

$$
\begin{aligned}
&= \frac{1}{2\pi}\left(\int_{-\pi}^{\pi}|A(\omega)|^2d\omega+\int_{-\pi}^{\pi}|D(\omega)|^2d\omega\right)\\
&= \frac{1}{4\pi}\left[\int_{-\pi}^{\pi}\left((|H(\frac{\omega}{2})|^2+|G(\frac{\omega}{2})|^2)|S(\frac{\omega}{2})|^2\right.\right.\\
&\quad +(|H(\frac{\omega}{2}+\pi)|^2+|G(\frac{\omega}{2}+\pi)|^2)|S(\frac{\omega}{2}+\pi)|^2\Big)\,d\omega\\
&\quad \left.+2\int_{-\pi}^{\pi}\mathrm{Re}\left((\overline{H(\frac{\omega}{2})}H(\frac{\omega}{2}+\pi)+\overline{G(\frac{\omega}{2})}G(\frac{\omega}{2}+\pi))S(\frac{\omega}{2})\overline{S(\frac{\omega}{2}+\pi)}\right)d\omega\right]\\
&\le \frac{1}{2\pi}\int_{-\pi/2}^{\pi/2}\left(|H(\omega)|^2+|G(\omega)|^2\right)|S(\omega)|^2d\omega\\
&\quad +\frac{1}{2\pi}\int_{-\pi/2}^{\pi/2}\left(|H(\omega+\pi)|^2+|G(\omega+\pi)|^2\right)|S(\omega+\pi)|^2d\omega\\
&\quad +\frac{1}{4\pi}\int_{-\pi}^{\pi}\left|\mathrm{Re}\left((\overline{H(\frac{\omega}{2})}H(\frac{\omega}{2}+\pi)+\overline{G(\frac{\omega}{2})}G(\frac{\omega}{2}+\pi)\right)\right|\left(|S(\frac{\omega}{2})|^2+|\overline{S(\frac{\omega}{2}+\pi)}|^2\right)d\omega\\
&= \frac{1}{2\pi}\int_{-\pi}^{\pi}\left(|H(\omega)|^2+|G(\omega)|^2\right)|S(\omega)|^2d\omega\\
&\quad +\frac{1}{2\pi}\int_{-\pi/2}^{\pi/2}\left|\mathrm{Re}\left((\overline{H(\omega)}H(\omega+\pi)+\overline{G(\omega)}G(\omega+\pi)\right)\right|\left(|S(\omega)|^2+|\overline{S(\omega+\pi)}|^2\right)d\omega\\
&\le C_{\max}\frac{1}{2\pi}\int_{-\pi}^{\pi}|S(\omega)|^2d\omega\\
&= C_{\max}\sum_n|s(n)|^2.
\end{aligned}
$$

□

A.3 Proof of Proposition 6:

It is clear from the discussion in Section 2 that $b_{j,k}=2^{-J/2}b_{j,k}^{(S)}$, $j<J, k\in\mathbf{Z}$, if and only if

$$c_{J,k}=2^{-J/2}x'[k],\ k\in\mathbf{Z}.$$

Therefore, we only need to prove that the above equation is equivalent to the condition (5.3). To do so, we examine what $2^{-J/2}x'[k]$ is.

$$
\begin{aligned}
2^{-J/2}x'[k] &= 2^{-J/2}\sum_m x[m]q[k-m]\\
&= 2^{-J/2}\int_{-\infty}^{\infty}\chi(t)\sum_m\phi(t-(k-m))x[m]dt\\
&= 2^{-J/2}\int_{-\infty}^{\infty}\chi(t)\sum_m\phi(t-(k-m))\frac{1}{2\pi}\int_{-\infty}^{\infty}\hat{f}(-\omega)e^{-i\omega m/2^J}d\omega dt\\
&= 2^{J/2}\int_{-\infty}^{\infty}\chi(t)\sum_m\frac{1}{2\pi}\int_{-\infty}^{\infty}\hat{\phi}(\omega_1)e^{i\omega_1(t-(k-m))}d\omega_1\frac{1}{2\pi}\int_{-\infty}^{\infty}\hat{f}(-2^J\omega)e^{-i\omega m}d\omega dt\\
&= \frac{2^{J/2}}{2\pi}\int_{-\infty}^{\infty}\hat{f}(-2^J\omega)\int_{-\infty}^{\infty}\chi(t)\int_{-\infty}^{\infty}\hat{\phi}(\omega_1)e^{i\omega_1(t-k)}\frac{1}{2\pi}\sum_m e^{im(\omega_1-\omega)}d\omega_1 dtd\omega
\end{aligned}
$$

$$
\begin{aligned}
&= \frac{2^{J/2}}{2\pi}\int_{-\infty}^{\infty}\hat{f}(-2^J\omega)\int_{-\infty}^{\infty}\chi(t)\int_{-\infty}^{\infty}\hat{\phi}(\omega_1)e^{i\omega_1(t-k)}\sum_m\delta(\omega_1-(\omega-2m\pi))d\omega_1 dt d\omega \\
&= \frac{2^{J/2}}{2\pi}\int_{-\infty}^{\infty}\hat{f}(-2^J\omega)\int_{-\infty}^{\infty}\chi(t)\sum_m\hat{\phi}(\omega+2m\pi)e^{i(\omega+2m\pi)(t-k)}dt d\omega \\
&= \frac{2^{J/2}}{2\pi}\int_{-\infty}^{\infty}\hat{f}(-2^J\omega)\sum_m\hat{\phi}(\omega+2m\pi)\int_{-\infty}^{\infty}\chi(t)e^{i(\omega+2m\pi)t}dt e^{-ik\omega}d\omega \\
&= \frac{2^{J/2}}{2\pi}\int_{-\infty}^{\infty}\hat{f}(-2^J\omega)\left[\sum_m\hat{\phi}(\omega+2m\pi)\hat{\chi}(-\omega-2m\pi)\right]e^{-ik\omega}d\omega \\
&= \frac{2^{J/2}}{2\pi}\int_{-\infty}^{\infty}\hat{f}(-2^J\omega)\left[\sum_m\hat{\phi}(\omega+2m\pi)\frac{\hat{\tilde{\phi}}(-\omega-2m\pi)}{\tilde{\Phi}(-\omega-2m\pi)}\right]e^{-ik\omega}d\omega \\
&= \frac{2^{J/2}}{2\pi}\int_{-\infty}^{\infty}\hat{f}(-2^J\omega)\left[\frac{\sum_m\hat{\phi}(\omega+2m\pi)\hat{\tilde{\phi}}(-\omega-2m\pi)}{\tilde{\Phi}(-\omega)}\right]e^{-ik\omega}d\omega \\
\text{by } &\overset{(2.3)}{=} \frac{2^{J/2}}{2\pi}\int_{-\infty}^{\infty}\hat{f}(-2^J\omega)\frac{1}{\tilde{\Phi}(-\omega)}e^{-ik\omega}d\omega.
\end{aligned}
$$

For the form of $c_{J,k}$, we refer to the proof of Proposition 1. Thus, condition (5.3) is equivalent to $c_{J,k} = 2^{-J/2}x'[k]$ and Proposition 6 is proved. □

A.4 Proof of Proposition 7:

$f(t) \in \tilde{V}_J$ implies, by Proposition 5,

$$f(t) = \sum_n f(\frac{n}{2^J})\chi(2^Jt-n) \triangleq f'(t).$$

Then

$$
\begin{aligned}
c_{J,k} &= \int_{-\infty}^{\infty} f(t)\phi_{Jk}(t)dt \\
&= \int_{-\infty}^{\infty}\sum_n x[n]\chi(2^Jt-n)2^{J/2}\phi(2^Jt-k)dt \\
&= 2^{-J/2}\sum_n x[n]\int_{-\infty}^{\infty}\chi(t-n)\phi(t-k)dt \\
&= 2^{-J/2}\sum_n x[n]q[k-n] = 2^{-J/2}x'[k].
\end{aligned}
$$

By using the same proof given in Proposition 6, we prove the fact that $f(t)$ satisfies (5.3).

On the other hand, even though condition (5.3) implies $f_J(t) = f'(t)$ as proved in Proposition 6, we do not have $f'(t) = f(t)$ in general. Thus, (5.3) does not guarantee $f(t) = f_J(t)$. This proves the second part of Proposition 7. □

A.5 Proof of Proposition 9:

Since $\|f - f'\| \leq \|f - f_J\| + \|f_J - f'\|$ and a bound for the term $\|f - f_J\|$ is given in Proposition 8, we only have to estimate the bound for $\|f_J - f'\|$ below. Due to (2.6) and that $\{\chi(2^J t - n)\}_n$ is a basis of $\tilde{V}_J$ (see Walter [31]), we know that both $f_J(t)$ and $f'(t)$ are in $\tilde{V}_J$. Therefore, by (2.14),

$$\begin{aligned}
\|f_J - f'\|^2 &= \int_{-\infty}^{\infty} \left| \sum_k (c_{J,k} - 2^{-J/2} x'[k]) \tilde{\phi}_{J,k}(t) \right|^2 dt \\
&= \frac{1}{2\pi} \int_{-\infty}^{\infty} \left| \sum_k (c_{J,k} - 2^{-J/2} x'[k]) e^{-ik\omega} \right|^2 |\hat{\tilde{\phi}}(\omega)|^2 d\omega \\
&= \frac{1}{2\pi} \int_{-\pi}^{\pi} \left| \sum_k (c_{J,k} - 2^{-J/2} x'[k]) e^{-ik\omega} \right|^2 \sum_k |\hat{\tilde{\phi}}(\omega + 2k\pi)|^2 d\omega \\
&\leq (C_1)^2 \frac{1}{2\pi} \int_{-\pi}^{\pi} \left| \sum_k (c_{J,k} - 2^{-J/2} x'[k]) e^{-ik\omega} \right|^2 d\omega \\
&= (C_1)^2 \sum_k |c_{J,k} - 2^{-J/2} x'[k]|^2,
\end{aligned}$$

where the second and last equalities are due to the Parseval Theorem. By the form of $c_{J,k}$ in the proof of Proposition 1 and the form of $x'[k]$ in the proof of Proposition 6, Proposition 9 is proved. □

A.6 Proof of Proposition 10:

Since $f_J(t) \in \tilde{V}_J$, we know by Proposition 5 that

$$f_J(t) = \sum_k f_J(\frac{k}{2^J}) \chi(2^J t - k).$$

Therefore,

$$\begin{aligned}
f_J(t) - f'(t) &= \sum_k (f_J(\frac{k}{2^J}) - f(\frac{k}{2^J})) \chi(2^J t - k) \\
&= \frac{1}{2\pi} \int_{-\infty}^{\infty} \hat{\chi}(\omega) e^{i2^J t\omega} \sum_k (f_J(\frac{k}{2^J}) - f(\frac{k}{2^J})) e^{-ik\omega} d\omega.
\end{aligned}$$

Let

$$\begin{aligned}
F_J(\omega) &= \sum_k (f_J(\frac{k}{2^J}) - f(\frac{k}{2^J})) e^{-ik\omega} \\
&= 2^J \sum_k (\hat{f}_J(2^J(\omega + 2k\pi)) - \hat{f}(2^J(\omega + 2k\pi))).
\end{aligned}$$

Therefore,

$$\begin{aligned}\int_{-\pi}^{\pi}|F_J(\omega)|^2d\omega &\leq 2^{2J}\sum_k\int_{-\pi}^{\pi}|\hat{f}_J(2^J(\omega+2k\pi))-\hat{f}(2^J(\omega+2k\pi))|^2d\omega\\ &= 2^{2J}\int|\hat{f}_J(2^J\omega)-\hat{f}(2^J\omega)|^2d\omega\\ &= 2^J\|\hat{f}_J-\hat{f}\|^2\\ &= 2\pi 2^J\|f_J-f\|^2.\end{aligned}$$

Going back to $f_J(t)-f'(t)$, we have

$$f_J(t)-f'(t)=\frac{1}{2\pi 2^J}\int_{\infty}^{\infty}\frac{\hat{\bar{\phi}}(\frac{\omega}{2^J})}{\hat{\Phi}(\frac{\omega}{2^J})}F_J(\frac{\omega}{2^J})e^{it\omega}d\omega.$$

Thus, applying the Parsevel theorem, we have

$$\begin{aligned}\|f_J-f'\|^2 &= \frac{1}{2\pi 2^{2J}}\int_{\infty}^{\infty}|\frac{\hat{\bar{\phi}}(\frac{\omega}{2^J})}{\hat{\Phi}(\frac{\omega}{2^J})}|^2|F_J(\frac{\omega}{2^J})|^2d\omega\\ &= \frac{1}{2\pi 2^J}\int_{\infty}^{\infty}|\frac{\hat{\bar{\phi}}(\omega)}{\hat{\Phi}(\omega)}|^2|F_J(\omega)|^2d\omega\\ &= \frac{1}{2\pi 2^J}\sum_k\int_{-\pi}^{\pi}\frac{|\hat{\bar{\phi}}(\omega+2k\pi)|^2}{|\hat{\Phi}(\omega)|^2}|F_J(\omega)|^2d\omega\\ &= \frac{1}{2\pi 2^J}\int_{-\pi}^{\pi}\frac{\sum_k|\hat{\bar{\phi}}(\omega+2k\pi)|^2}{|\hat{\Phi}(\omega)|^2}|F_J(\omega)|^2d\omega\\ &\leq C_2^2\|f_J-f\|^2.\end{aligned}$$

where

$$C_2=\max_{\omega\in[-\pi,\pi]}\frac{(\sum_k|\hat{\bar{\phi}}(\omega+2k\pi)|^2)^{1/2}}{|\hat{\Phi}(\omega)|}=\max_{\omega\in[-\pi,\pi]}\left(\frac{\hat{\bar{\phi}}(\omega)}{\hat{\phi}(\omega)}\right)^{1/2}\frac{1}{|\hat{\Phi}(\omega)|}.$$

Therefore,

$$\|f-f'\|\leq\|f-f_J\|+\|f_J-f'\|\leq\|f-f_J\|(1+C_2).$$

Combining Proposition 8, Proposition 10 is proved. □

References

[1] M. Antonin, M. Barlaud, P. Mathieu, and I. Daubechies, "Image coding using vector quantization in the wavelet transform domain," in *IEEE Proceedings of ICASSP*, (Albuquerque, New Mexico), pp. 2297–2300, 1990.

[2] N. Baaziz and C. Labit, "Laplacian pyramid versus wavelet decomposition for image sequence coding," in *IEEE Proceedings of ICASSP*, (Albuquerque, New Mexico), pp. 1965–1968, 1990.

[3] M. Basseville, A. Benveniste, K. C. Chou, S. A. Golden, R.Nikoukhah, and A. S. Willsky, "Modeling and estimation of multiresolution stochastic processes," *IEEE Trans. on Information Theory*, Vol. 38, pp. 766–784, Mar. 1992.

[4] G. Beylkin, R. Coifman, and V. Rokhlin, "Fast wavelet transform and numerical algorithm I," *Comm. Pure and Applied Math.*, Vol. 44, pp. 141–183, 1991.

[5] C. K. Chui, *An Introduction to Wavelets*, New York: Academic Press, 1992.

[6] C. K. Chui, ed., *Wavelets: A Tutorial in Theory and Applications*, New York: Academic Press, 1992.

[7] A. Cohen, "Biorthogonal wavelets," in *Wavelets: A Tutorial in Theory and Applications* (C. K. Chui, ed.), pp. 123–152, New York: Academic Press, 1992.

[8] J. M. Combes, A. Grossmann, and P. Tchamitchian, eds., *Wavelets, Time-Frequency Methods and Phase Space*, Berlin: Springer, IPTI, 1989.

[9] I. Daubechies, "Orthonormal bases of compactly supported wavelets," *Comm. on Pure and Appl. Math.*, Vol. 41, pp. 909–996, 1988.

[10] I. Daubechies, "The wavelet transform, time-frequency localization and signal analysis," *IEEE Trans. on Information Theory*, Vol. 36, pp. 961–1005, Sept. 1990.

[11] S. Golden, "Identifying Multiscale Statistical Models Using the Wavelet Transform," tech. rep., MIT, Dept. of Elec. Eng. and Comp. Science. SM Thesis.

[12] P. Goupillaud, A.Grossmann, and J.Morlet, "Cycle-octave and related transforms in seismic signal analysis," *Geoexploration*, Vol. 23, pp. 85–102, 1984/85.

[13] C. E. Heil and D. F. Walnut, "Continuous and discrete wavelet transform," *SIAM Review*, Vol. 31, pp. 628–666, Dec. 1989.

[14] M. Holschneider, R. Kronland-Martinet, J. Morlet, and P. Tchamitchian, "A real-time algorithm for signal analysis with the help of the wavelet transform," in *Wavelets, Time-Frequency Methods and Phase Space* (A. G. J.M. Combes and P. Tchamitchian, eds.), pp. 286–297, Berlin: Springer, IPTI, 1989.

[15] S. Jaffard and P. Laurençt, "Orthonormal wavelets, analysis of operators, and applications to numerical analysis," in *Wavelets: A Tutorial in Theory and Applications* (C. K. Chui, ed.), pp. 543–601, New York: Academic Press, 1992.

[16] J. Kovačevič and M. Vetterli, "Nonseparable multidimensional perfect reconstruction banks and wavelet for $\mathcal{R}$n," *IEEE Trans. on Information Theory*, Vol. 38, pp. 533–555, Mar. 1992.

[17] A. Latto and E. Tenenbaum, "Compactly supported wavelets and the numerical solution of Burgers' equation," *C. R. Acad. Sci. France, Série I*, pp. 903–909, 1990.

[18] S. Mallat, "Multifrequency channel decompositions of images and wavelet methods," *IEEE Trans. on Acoustics, Speech and Signal Processing*, Vol. 37, pp. 2091–2110, 1989.

[19] S. Mallat, "Multiresolution approximations and wavelet orthonormal bases of $L^2(R)$," *Trans. Amer. Math. Soc.*, Vol. 315, pp. 69–87, Sept. 1989.

[20] S. Mallat, "A theory for multiresolution signal decomposition: the wavelet representation," *IEEE Trans. on Pattern Anal. and Mach.Intell.*, Vol. 11, pp. 674–693, 1989.

[21] Y. Meyer, *Ondelettes et Operateurs*, Paris, France: Hermann, 1990.

[22] T. Paul and K. Seip, "Wavelets and quantum mechanics," in *Wavelets and Their Applications* (R. et al, ed.), pp. 303–322, Boston: Jones and Bartlett, 1992.

[23] O. Rioul and P. Duhamel, "Fast algorithms for discrete and continuous wavelet transform," *IEEE Trans. on Information Theory*, Vol. 38, pp. 569–586, Mar. 1992.

[24] O. Rioul and M. Vetterli, "Wavelets and signal processing," *IEEE Signal Processing Magazine*, pp. 14–38, Oct. 1991.

[25] M. J. Shensa, "Affine wavelets: Wedding the Atrous and Mallat algorithms," *IEEE Trans. on Signal Processing.* to appear.

[26] G. Strang, "Wavelets and dilation equations: A brief introduction," *SIAM Review*, Vol. 31, pp. 614–627, 1989.

[27] F. Tuteur, "Wavelet transformations in signal detection," in *IEEE Proceedings of ICASSP*, (New York), pp. 1435–1438, April 1988.

[28] M. Unser and A. Aldroubi, "Polynomial splines and wavelets–A signal processing perspective," in *Wavelets: A Tutorial in Theory and Applications* (C. K. Chui, ed.), pp. 91–122, New York: Academic Press, 1992.

[29] P. P. Vaidyanathan, "Multirate digital filters, filter banks, polyphase networks, and applications: A tutorial," *Proc.IEEE*, Vol. 78, pp. 56–93, Jan. 1990.

[30] M. Vetterli and C. Herley, "Wavelets and filter banks: Theory and design," *IEEE Trans. Signal Processing.* to appear.

[31] G. G. Walter, "A sampling theorem for wavelet subspace," *IEEE Trans. on Information Theory*, Vol. 38, pp. 881–884, Mar. 1992.

[32] G. W. Wornell, "A Karhunen-Loève-like expansion for $1/f$ processes via wavelets," *IEEE Trans. on Information Theory*, Vol. 36, pp. 859–861, July 1991.

[33] G. W. Wornell and A. V. Oppenheim, "Estimation of fractal signals from noisy measurements using wavelets," *IEEE Trans. on Signal Processing*, Vol. 40, pp. 611–623, Mar. 1992.

[34] X. G. Xia, C.-C. J. Kuo, and Z. Zhang, "Design of optimal FIR prefilters for wavelet coefficient computation," *IEEE Trans. on Circuits and Systems-II*, 1992. Submitted.

[35] X. G. Xia, C.-C. J. Kuo, and Z. Zhang, "On the accuracy of computed wavelet coefficients," *SIAM J. on Numerical Analysis*, 1992. Submitted.

[36] X. G. Xia and Z. Zhang, "Error estimation and wavelet choice in wavelet series approximation," *IEEE Trans. on Information Theory*, 1992. Submitted.

Figure Captions

Figure 1: (a) $|H(\omega)|^2 + |G(\omega)|^2$ and (b) Re $\Big((\overline{H(\omega)}H(\omega+\pi) + \overline{G(\omega)}G(\omega+\pi)\Big)$.

Figure 2: The errors e_5, e_4 and e_3 between desired $b_{j,k}$ and computed $b_{j,k}^{(S)}$. (a): The optimal prefilters are signal dependent in Table 1; (b): The optimal prefilters are signal independent in Table 2.

Figure 3: $\chi_o(t)$ corresponding to the optimal prefilters $q_o[n]$ in Tables 1-2. (a): for $q_o[n]$ with length $N_1 = 1$ in Table 1; (b): for $q_o[n]$ with length $N_1 = 1$ in Table 2; (c): for $q_o[n]$ with length $N_1 = 2$ in Table 1; (d): for $q_o[n]$ with length $N_1 = 2$ in Table 2.

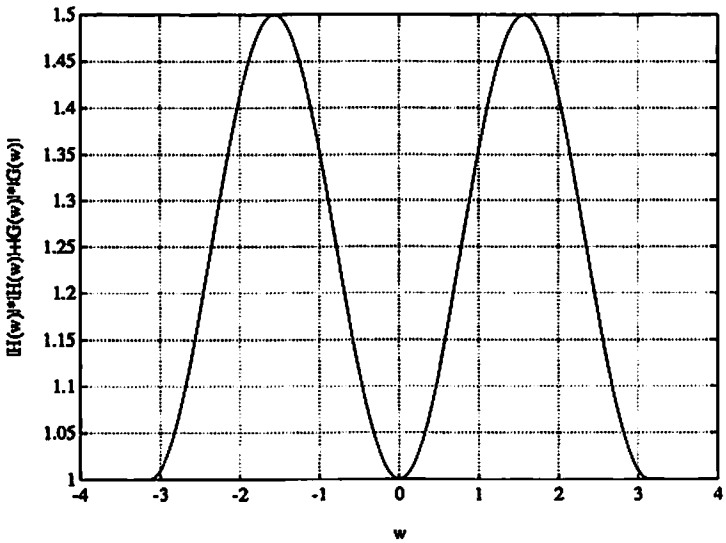

(*a*)

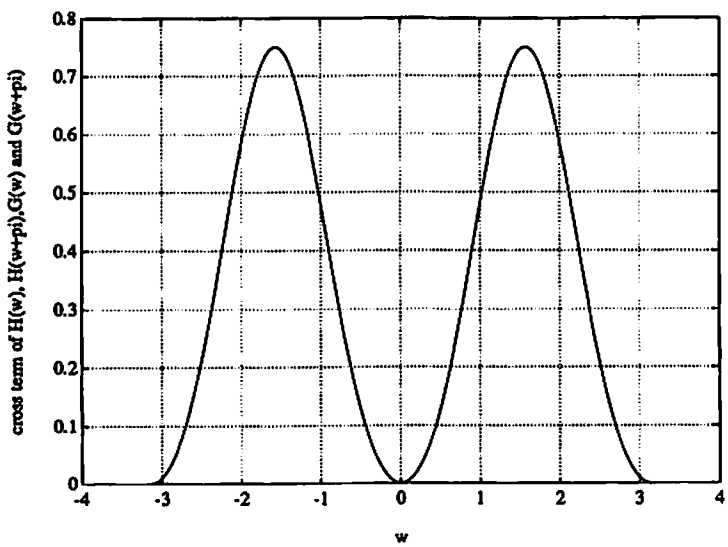

(*b*)

Figure 1: (a) $|H(\omega)|^2 + |G(\omega)|^2$ and (b) $\mathrm{Re}\left((\overline{H(\omega)}H(\omega+\pi) + \overline{G(\omega)}G(\omega+\pi)\right)$.

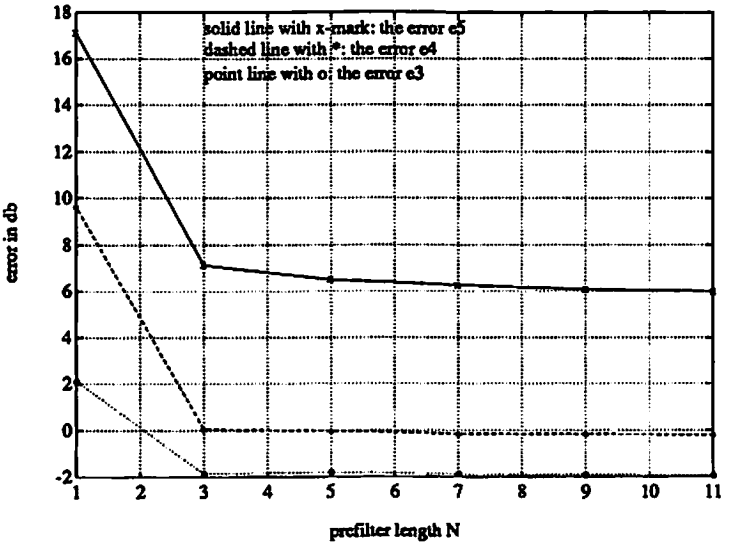

(a)

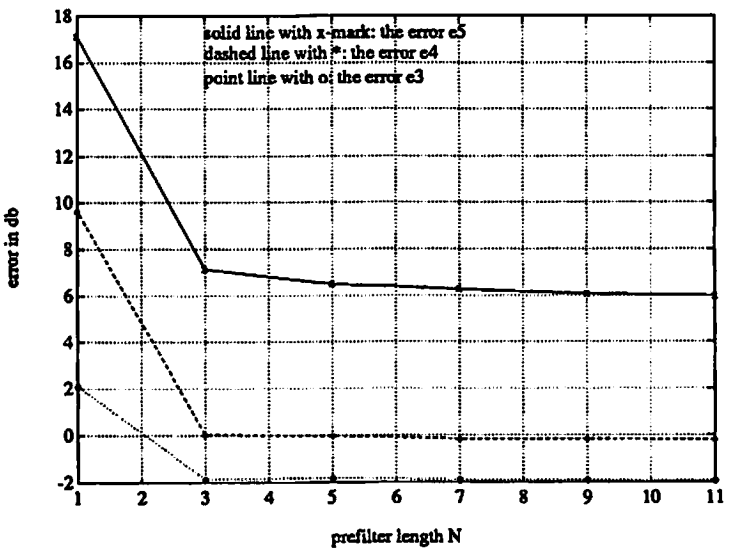

(b)

Figure 2: The errors e_5, e_4 and e_3 between desired $b_{j,k}$ and computed $b_{j,k}^{(S)}$. (a): The optimal prefilters are signal dependent in Table 1; (b): The optimal prefilters are signal independent in Table 2.

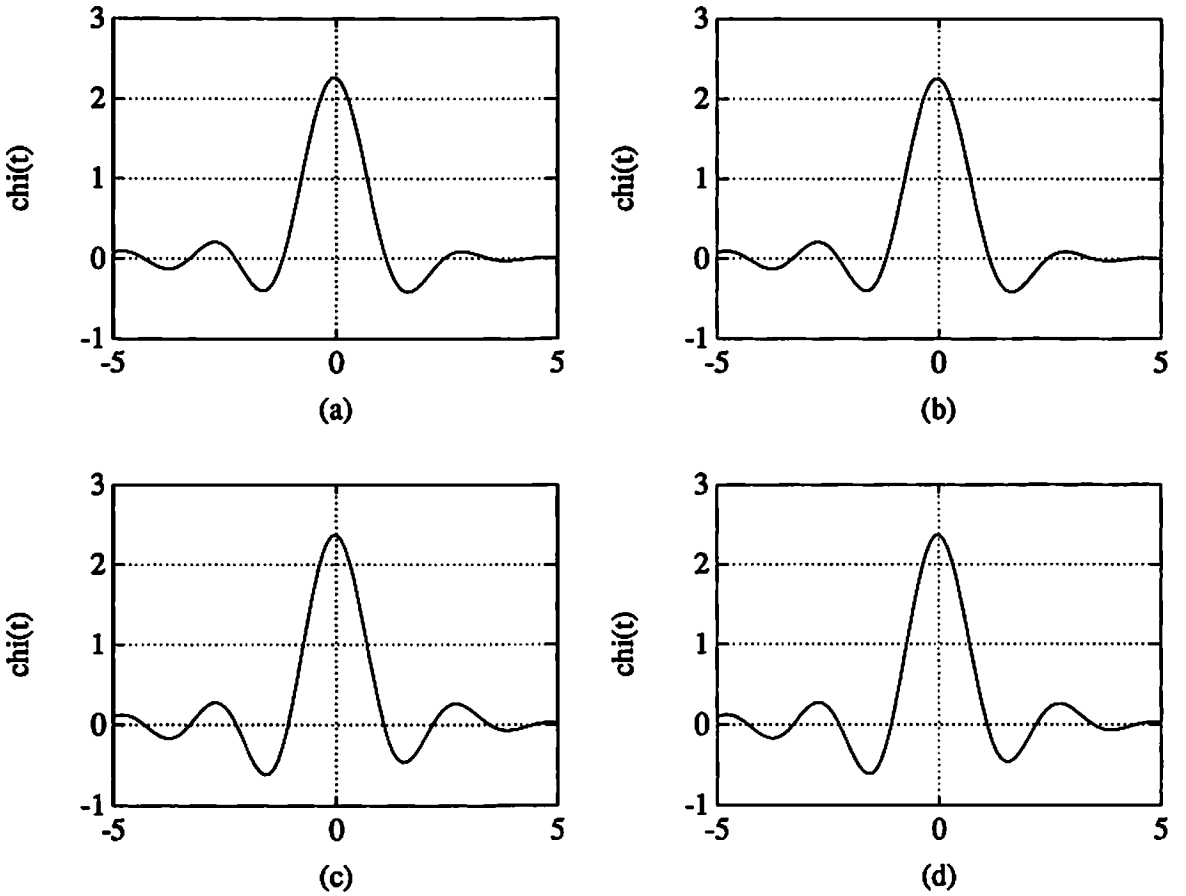

Figure 3: $\chi_o(t)$ corresponding to the optimal prefilters $q_o[n]$ in Tables 1-2. (a): for $q_o[n]$ with length $N_1 = 1$ in Table 1; (b): for $q_o[n]$ with length $N_1 = 1$ in Table 2; (c): for $q_o[n]$ with length $N_1 = 2$ in Table 1; (d): for $q_o[n]$ with length $N_1 = 2$ in Table 2.